Astron. Astrophys. 240, 289–298 (1990)

ASTRONOMY AND ASTROPHYSICS

Generation and interpretation of galactic magnetic fields

K. J. Donner and A. Brandenburg

Observatory and Astrophysics Laboratory, University of Helsinki, Tähtitorninmäki, SF-00130 Helsinki, Finland

Received April 5; accepted July 31, 1990

Abstract. We present kinematic mean-field dynamo models for galaxies consisting of a turbulent gas disc embedded in a low-conductivity spherical halo. In the cases investigated an axisymmetric mode is the dominant one. This mode can be of either even or odd parity (S0 or A0, respectively). The preference of S0 or A0 modes is governed mainly by the radial profiles of the α effect and the turbulent magnetic diffusivity. If the gas disc extends into the galactic centre, the dominant mode is of A0 type and it is concentrated within the central region. If the model is changed so that induction effects are absent in the centre, the dominant mode is an axisymmetric spiral of even parity. We point out that a finite disc thickness and a low-conductivity halo will both lead to appreciable vertical magnetic fields outside the disc plane, and this may affect the interpretation of polarisation observations. We integrate the transfer equations for the three Stokes parameters I, Q, and U and produce in this way synthetic maps for the observed polarisation and rotation measures. Assuming a disc-like distribution of relativistic electrons, our models suggest that for moderate disc thickness modifications of the observed polarised emission due to fields above the plane are minor. For more extended electron distributions quite complicated polarisation patterns are obtained. Still, qualitatively the criteria distinguishing axisymmetric and bisymmetric spiral patterns remain valid.

Key words: galaxies: magnetic fields – hydromagnetics: disc dynamos – polarisation – Faraday rotation

1. Introduction

In recent years there have been remarkable improvements in the observations of galactic magnetic fields (Sofue et al., 1988, Beck, 1990). For nearby spiral galaxies maps are available at several wavelengths showing distributions of total and polarised synchrotron intensity over galactic discs with a resolution that is good enough to distinguish spiral arms and other detailed features. The interpretation of the observations in terms of actual magnetic fields is a complex problem involving incompletely known distributions of thermal and cosmic-ray electrons. Ideally, one would like to infer the complete magnetic field structure from the observed maps. In practice, one usually interprets the observed polarisation maps in terms of some simple field configuration neglecting, for example, the finite field extension into the galactic halo. As the quality of the observations improves it becomes possible to compare the observations with more specific models. In this paper we take the first steps in this direction by computing synthetic observational maps using field configurations derived from mode calculations for realistic models incorporating a turbulent galactic disc embedded in a conducting halo.

Starting with the early work of Parker (1971), most previous dynamo models for galaxies (e.g. Baryshnikova et al., 1987; Ruzmaikin et al., 1988a,b; Krasheninnikova et al., 1990; Sawa & Fujimoto 1986; Fujimoto & Sawa 1987) have been based on the thin-disc approximation. However, one cannot be sure that the eigenvalues of these models are representative for discs with a finite radial extension (Rädler & Bräuer, 1987; Krause, 1990). In the thin-disc approximation the vertical magnetic field is very small. Previous interpretations of the magnetic field structure have been based on the modes computed from disc dynamo theory, and have therefore neglected any vertical fields.

In our models we avoid the assumptions inherent to the thin-disc approximation. We present dynamo models taking finite disc thickness and halo conductivity into account. We follow the procedure of embedding the galactic disc in a spherical domain of small, but finite conductivity (Stepinski & Levy, 1988; Elstner et al., 1990; Brandenburg et al., 1990). On the boundary of this spherical domain we can adopt the usual vacuum boundary condition. In this way we can compute the complete set of modes, without the *a priori* assumptions made in thin-disc theory.

There are observational reasons to doubt the assumptions made in the thin-disc models. The most recent determination of the scale height of free electrons in the Galaxy is about 1.5 kpc (Reynolds, 1989). The close correlation between synchrotron emission and the light from old disc stars noted by Allen et al. (1990) also argues in favour of models with thicker discs. Furthermore, in edge-on galaxies ordered magnetic fields are found to extend to considerable heights above the disc (Hummel et al., 1988).

A particularly important result of the observations is that the magnetic field in galaxies may be either an axisymmetric (Krause et al., 1989a) or a bisymmetric (Krause et al., 1989b) spiral, denoted henceforth as ASS or BSS, respectively. This poses a considerable difficulty for kinematic dynamo models. Axisymmetric modes are dominant already in α^2 dynamos, and the problem is usually aggravated by differential rotation, since realistic profiles for the angular velocity typically lead to a winding up of field lines in such a manner that non-axisymmetric

Send offprint requests to: K. J. Donner fields are effectively dissipated (Rädler, 1986; Brandenburg et al., 1990). In consequence, axisymmetric spirals (ASS) are usually the dominant field structures in kinematic models.

So far, it has been possible to obtain dominant modes with non-axisymmetric field configurations only with very strong anisotropies of the α effect (Krause et al., 1990). Another possibility, which has not been investigated in detail (see however Mestel & Subramanian 1990, Chiba & Tosa 1990), would be an α effect with a spiral distribution. One may also speculate that non-axisymmetric fields are possible in a sufficiently nonlinear regime via secondary bifurcations (cf. Jennings et al., 1990). For nonlinear dynamos with flat α effect distribution complicated mixed-parity solutions have been found (Moss & Tuominen, 1990), but here only axisymmetric fields have been computed.

A further problem is how the field near the centre of the Milky Way, which can be seen in jet-like streaks pointing out of the galactic plane (Sofue et al., 1989, Yusef-Zadeh et al., 1984, 1986), is related to the field in the main part of the disc. The question is whether such field configurations can be caused by a dynamo process. Donner (1990) noted that the present models give rise to an α^2 dynamo generated A0 mode that is strongly concentrated toward the centre.

Let us now return to the interpretation of observations. In galaxies one has the advantage in contrast to solar dynamo theory that one can look directly into the galaxy. Employing polarisation measurements it is possible to determine the magnetic field orientation inside the galaxy. However, one can only observe the integrated emission along the line of sight. In practice the measured Stokes parameters I, Q, and U contain contributions from all distances. If galactic magnetic fields extend far into the galactic halo, this may give considerable contributions to the integrated Stokes parameters, which should be taken into account, as has also been stressed by Sawa & Fujimoto (1986).

An important diagnostic quantity is the rotation measure RM. In the pioneering work of Tosa & Fujimoto (1978) a method was introduced to determine whether the field was ASS or BSS by plotting the variation of RM around a circle of constant radius in the plane of the galaxy. However, these authors based their argument on the assumption that the magnetic field is oriented parallel to the disc. This is likely to be a good approximation if the $\alpha\omega$ mechanism dominates, and is also true in the thin-disc approximation (Baryshnikova et al., 1987). Nevertheless, in general there will be a vertical field component, and its effect on the interpretation of observations needs to be considered. In our models the vertical field is not small, and it is therefore important to study the effect on the resulting distribution of polarisation measures.

In the present paper we also consider non-axisymmetric field configurations, although they do *not* represent the dominant mode. Our purpose here is to investigate the effect of extended field structures on the interpretation of observations. We expect that the non-axisymmetric field configurations will basically depend on the structure of the turbulent disc. Thus, although we cannot explain a preference for non-axisymmetric fields, we feel that our computed field structures are more realistic than the rather schematic fields considered sometimes in the literature (e.g. logarithmic spirals). It allows us in particular to estimate the contributions to the integrated Stokes parameters due to the field extension into the galactic halo.

This paper is organised as follows. In the following section we specify the model and in Sect. 3 we discuss the results as regards the field configuration. Implications for the interpretation of observed polarisation maps are presented in Sect. 4 and our conclusions are given in the last section.

2. Models and methods

The time-development of the mean magnetic field $\boldsymbol{B}$ is governed by the induction equation

$$\frac{\partial \boldsymbol{B}}{\partial t} = \mathrm{curl}\,(\boldsymbol{u} \times \boldsymbol{B} + \alpha \boldsymbol{B} - \eta\,\mathrm{curl}\,\boldsymbol{B}). \tag{1}$$

Spherical coordinates r, θ, ϕ are used. The mean velocity $\boldsymbol{u}$ is related to the angular velocity of differential rotation Ω according to $\boldsymbol{u} = \hat{\boldsymbol{\phi}}\Omega r \sin\theta$, where $\hat{\boldsymbol{\phi}}$ is the unit vector in the ϕ direction.

In our models a galaxy is characterised by a turbulent gas disc embedded in a low-conductivity halo. Our choice of model is based on the following considerations: Supernova explosions in the disc will give rise to extensive regions of hot ionised gas with a scale height of several kpc (McKee & Ostriker, 1977). Star formation and evolution in the disc will vigorously drive turbulent motions in the ionised gas near the disc plane giving rise to an effective α effect and turbulent diffusivity. The disc will be surrounded by a lower density corona. In the present paper we assume that some level of turbulence is maintained in the corona, yielding a turbulent diffusivity, but no α effect. This type of structure appears to be present in NGC 891, where several components in the electron distribution are observed (Rand et al., 1990).

To specify a model the angular velocity Ω, diffusivity η, and α effect have to be given as functions of r and θ. We neglect azimuthal dependences of the functions Ω, η, and α, but the magnetic field is allowed to be non-axisymmetric. The turbulent effects of the interstellar medium are incorporated in the coefficients α and η. At this stage we do not include any of the more complex turbulent effects (cf. Rädler, 1980). In particular, although the α effect is expected to be anisotropic in galaxies (Rüdiger, 1990), we restrict ourselves to an isotropic α. It should be stressed that the derivation of an equation for the mean field is generally based on a separation of large and small spatial or temporal scales. In galaxies, however, the turbulent length scale is likely to be of a similar order as the vertical gradients. We therefore view Eq. (1) as a simplified model equation incorporating in a qualitative way effects that are expected to be present on general grounds. Our concern in this paper is to investigate what magnetic fields are expected in the simplest mean-field dynamo models, without making assumptions about disc thickness and boundary conditions.

The angular velocity of differential rotation is taken to be

$$\Omega(\varpi) = \Omega_0 \left[1 + \left(\frac{\varpi}{\varpi_0}\right)^n\right]^{-1/n}, \tag{2}$$

where $\varpi = r\sin\theta$ is the distance from the axis. This gives a schematic representation of typical observed galactic rotation curves (Rubin et al., 1985). We assume that this rotation law applies also to the halo. For the turbulent diffusivity we assume

$$\eta(\varpi, z) = \begin{cases} \eta_0 - \eta_d(\varpi)\left[1 - \left(\dfrac{z}{z_0}\right)^2\right] & \text{if} \quad |z| \le z_0, \\ \eta_0 & \text{if} \quad |z| \ge z_0, \end{cases} \tag{3}$$

where $z = r\cos\theta$ is the distance from the equatorial plane, and z_0 the thickness of the disc. The turbulent diffusivity is thus a combination of a constant diffusivity η_0 representing the halo and a pure disc component η_d. For the α effect we take

$$\alpha(\varpi, z) = \begin{cases} \alpha_0(\varpi)\,\omega(\varpi)\,\dfrac{z}{z_0}\left[1-\left(\dfrac{z}{z_0}\right)^2\right] & \text{if} \quad |z| \le z_0, \\ 0 & \text{if} \quad |z| \ge z_0, \end{cases} \tag{4}$$

where $\omega(\varpi)$ represents a dimensionless vorticity profile curl $\boldsymbol{u}$ of the mean flow:

$$\Omega_0\,\omega(\varpi) = 2\Omega(\varpi) + \varpi\frac{d\Omega}{d\varpi}. \tag{5}$$

Expression (4) is based on the fact that α is (under certain assumptions) proportional to the local helicity which is the scalar product of the fluctuating parts of the velocity and vorticity. Assuming here that the fluctuating part of the vorticity is proportional to the mean vorticity, curl $\boldsymbol{u}$, we consider Eq. (4) as a reasonable ansatz. The vertical distribution of α should be antisymmetric and that of η should be symmetric with respect to the disc plane, but the functional form we have assumed is otherwise arbitrary. However, since both α and η are produced by the turbulence in the disc we shall assume that they have the same scale height z_0 and that the ϖ dependence of α_0 and η_d is the same.

The smallest diffusivity in the disc is $\eta^{\min} = \eta_0 - \eta_d^{\max}$. Reynolds numbers for the rotational velocity and the α effect can be defined based on the minimum diffusivity and on the halo radius L

$$R_\Omega = \Omega_0\,L^2/\eta^{\min}, \quad R_\alpha = \alpha_0^{\max}\,L/\eta^{\min}. \tag{6}$$

The coefficients α_0 and η_d are functions of radius, depending on the processes that are stirring the interstellar turbulence (stellar winds, supernovae etc.). In general one expects them to be related to the rate of star formation. On this basis we have considered two types of models for the radial distribution of turbulence, one in which the turbulent disc continues into the centre of the galaxy (model C), and another one in which we cut off the disc at an inner and at an outer radius (model R). In the first case we simply take α_0 and η_d to be constant. In the second case we impose a smooth inner and outer cutoff over a distance $0.1\,L$ using a fourth order polynomial. For this case we have used an inner radius of $0.5\,L$ and an outer radius of $0.7\,L$.

All the results given here will be for the parameter values $n = 2$, $\varpi_0 = 0.3\ L$, $z_0 = 0.2\ L$, $\eta_0/\eta^{\min} = 10$, and $R_\Omega = 1000$. Keeping in mind the observational uncertainties we feel that these values are representative for typical galaxies. For a detailed discussion of the relevant observations, see e.g. Ruzmaikin et al. (1988b, Chap. VI). We shall use the halo radius as unit of length, i.e. $L = 1$, and $L^2/\eta^{\min}$ as the unit of time.

We look for solutions of the induction equation (1) that are proportional to $\exp(-i\omega t + \lambda t + im\phi)$, where ω and λ are real coefficients and m is the order of the mode. These modes are classified as Sm (Am) according to whether the magnetic field is symmetric (antisymmetric) with respect to the equatorial plane.

The induction equation is solved numerically using the Bullard-Gellman formalism (Roberts & Stix, 1972). The field is written as the sum of a toroidal and a poloidal component, $\boldsymbol{B} = \text{curl}\,\text{curl}\,(\hat{\boldsymbol{r}}S) + \text{curl}\,(\hat{\boldsymbol{r}}T)$, where $\hat{\boldsymbol{r}}$ is the unit vector in the radial direction. The defining scalars S, T and the functions Ω, α and η are expanded in terms of Spherical Harmonics. Truncating these expansions at some level yields an eigenvalue problem for a set of ordinary differential equations, which is solved by a finite-difference method. Here we have used 50 gridpoints in the radial direction and 15 terms in the θ expansion. For further details of the numerical method, see Donner & Brandenburg (1990a) and references therein.

3. Magnetic field structure of the dynamo modes

As already reported by Donner (1990), the magnetic field configuration of the dominant modes will be qualitatively different depending on whether the α effect in the disc is allowed to continue into the galactic centre or not. In the case where the α effect is also active in the centre (model C), the dominant modes are generated essentially by an α^2 process. The differential rotation modifies the field geometry and the excitation conditions only slightly. The field is of A0 type, corresponding to a dipole field oriented along the rotation axis, and is confined to the central region.

On the other hand, in the ring model R in which α vanishes close to the centre the dominant modes are of S0 type. These modes extend over a large fraction of the disc and are similar to the modes calculated in the thin-disc approximation. For these modes the $\alpha\omega$ process is important and winding up of the magnetic field by differential rotation determines the field structure. For both models C and R the dominant modes tend to be concentrated in the region of maximum amplification, in agreement with the argument of Starchenko & Shukurov (1989).

We have *not* been able to find any cases where non-axisymmetric modes are preferred. This merely confirms the results of previous investigations. As explained in the Introduction we nevertheless study the field geometry of an S1 mode, because we do not expect dramatic differences in the field structure compared to the case where S1 is really preferred.

3.1. Magnetic fields at the galactic centre (model C)

We have found that the most simplified dynamo models predict a non-oscillatory axisymmetric dipolar field located at the centre of galaxies. The field configuration of this A0 mode for model C is shown in Fig. 1. In this case $R_\alpha = 120$ and the growth rate $\lambda = 18$. The left hand part shows the field in the meridional plane. On the right-hand side some field lines starting close to the centre are integrated outwards. Note the strong collimation of field lines.

In the first computations of global modes in flat configurations by Stix (1975) S0 modes were found to be preferred. However, the rotation curve used by Stix was very different from ours. It was noted by Donner & Brandenburg (1990b) that for S1 modes in the absence of an α effect the decaying modes of disc models may either be confined to the central rigidly rotating part of the disc or be more widely distributed. The occurrence of two geometrically distinct classes of modes appears to be related to the disc diffusivity, since Brandenburg et al. (1990) did not find similar behaviour in their models with a flat α distribution but spherical diffusivity. We now find that non-oscillatory A0 modes of the first type become dominant when the α effect is included. On the other hand, Stepinski & Levy (1988) using a rotation curve similar to ours found for their flat models oscillatory A0 solutions. They attributed the dominance of oscillatory fields

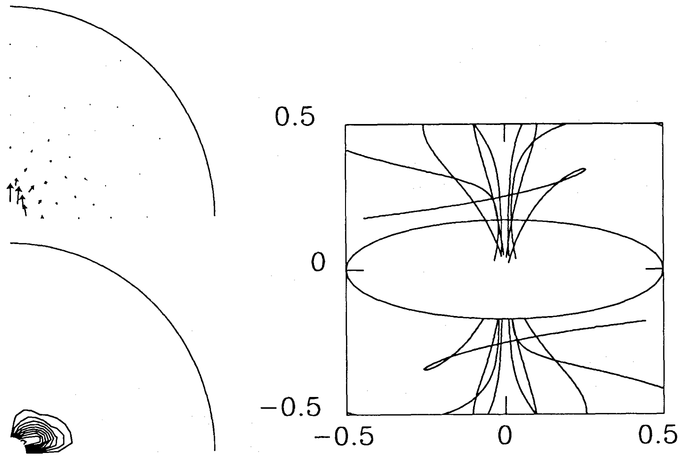

Fig. 1. Field configuration of the dominant A0 mode for model C. *Left*: field vectors of the meridional field (upper part) and contour levels of the azimuthal field (lower part) in a meridional plane. *Right*: field lines starting close to the centre are integrated outwards. The initial radii were $r = 0.05\,L$, the latitudes $\pm 45°$ and $\pm 75°$, and the longitudes 0°, 90°, 180°, and 270°. To show the position and inclination of the disc we have plotted a circle with radius $0.5\,L$ in the disc plane

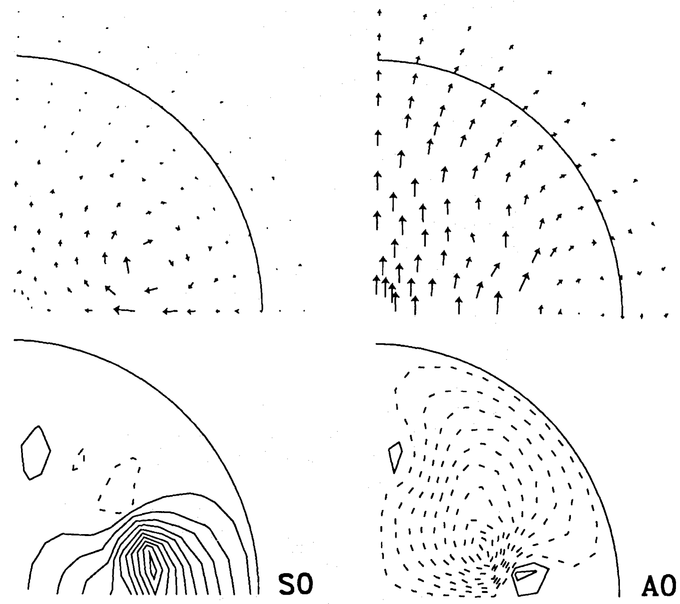

Fig. 2. Field configuration for the S0 and A0 modes for model R. In the upper row field vectors of the meridional field are plotted. The lower row shows contour levels of the azimuthal field component in a meridional plane. Dotted contours denote negative values

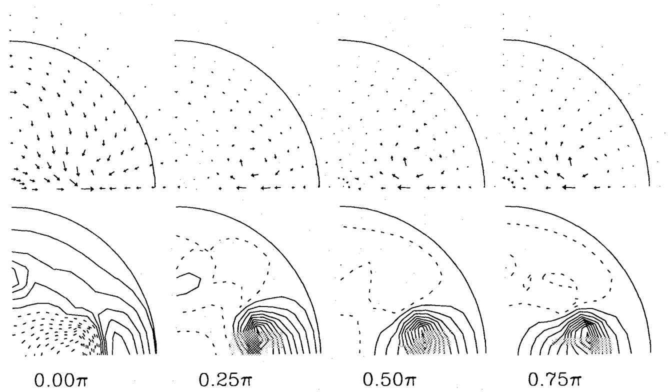

Fig. 3. Field configuration for the S1 mode for model R. The field is shown in four different meridional planes at azimuthal angles between 0 and $3\pi/4$. Otherwise as Fig. 2

to the thickness of the disc in their model. This explanation is supported by the results of Brandenburg et al. (1990, compare the upper two panels in their Fig. 3).

Observations of the centre of our galaxy show jet-like non-thermal emission both on a scale of about 30 pc (Yusef-Zadeh et al., 1984, 1986) and on a scale of a few kpc (Sofue et al., 1989). It has been argued by Yusef-Zadeh & Morris (1988) and Morris & Yusef-Zadeh (1989) that these observations indicate a pervasive dipolar field, which is not produced by activity in the galactic nucleus. The observations should be compared with the field lines of our central A0 mode, shown in the right hand part of Fig. 1. The field lines passing close to the centre are qualitatively similar to the observed jets, if these are interpreted as flux tubes traced by relativistic electrons injected by sources near the galactic centre. Of course, the observed field represents only one realisation of a random process, and it is not clear how well it can be expected to correspond to the theoretical mean field. Here we simply wish to stress that *the structure of observed central fields are in agreement with the predictions of simple dynamo models.* A detailed explanation of the field structure might still require more specific models such as that of Lesch et al. (1989).

3.2. Field structure for model R

We consider now the ring model in more detail. This is also the model that will be utilised in Sect. 4 for determining polarisation maps. The dominant mode is of type S0, but we also consider the first modes of type S1 and A0 for comparison. These modes have the growth rates 2, −48, and −96 respectively for $R_\alpha = 1000$. S0 and A0 are non-oscillatory and S1 rotates with angular velocity 464. The field configuration of the S0 and A0 modes are shown in Fig. 2. Note that the structure of the A0 mode may not be representative because of its rapid decay. We shall still include it for comparison in some of the figures.

For the S1 mode we have plotted the field in four different meridional planes for azimuthal angles between 0 and $3\pi/4$, see Fig. 3. The field vectors in the equatorial plane are shown in Fig. 4 for the S0 and S1 modes. It can be seen that S0 represents an axisymmetric spiral field whereas S1 is bisymmetric.

In order to illustrate the field configurations of the S0 and S1 modes further we have integrated field lines starting at radius 0.6 and 5°above and below the disc plane. The result is shown in Fig. 5. For the S0 mode, the field lines on each side of the plane form helices twisting around a central circular field line (not plotted). As the distance from the circular line increases, the helices become more tightly wrapped. In general the field lines are not closed and fill a surface enclosing the circular line. The field lines for S1 are more complex. Helical portions are interrupted by loops, where the field lines make large excursions into the halo.

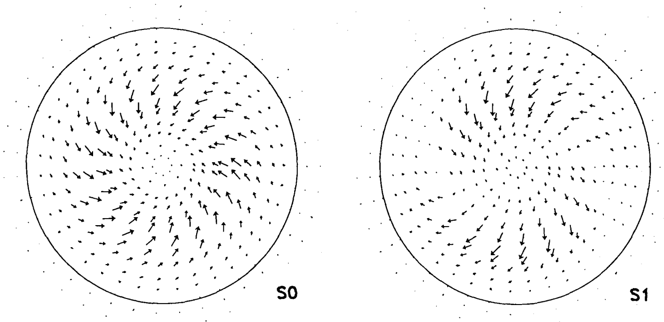

Fig. 4. Field vectors in the equatorial plane for the S0 and S1 modes of model R

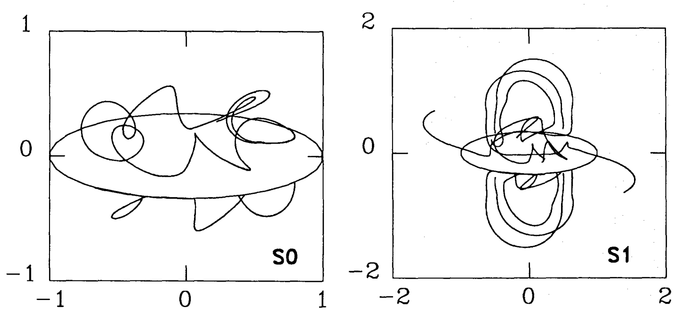

Fig. 5. Field lines for the S0 and S1 modes for model R. To show the position and inclination of the disc we have plotted a circle with radius unity in the disc plane. The integration of field lines has been terminated after a certain length. Field lines of S0 do *not* close after one revolution, i.e. they describe a rosette spiral. Note the different scales in the two panels

4. Polarised emission from thick discs

If the turbulent disc is thick and/or if the halo has a low conductivity the dynamo fields will have a considerable magnitude also high above the galactic plane. It is therefore not any longer justified to neglect the vertical field components and the vertical distribution of the field in the interpretation of polarisation observations. For some critical remarks on the customary methods of interpretation, see Heiles (1987). We are here concerned with the model with "empty" centre (model R).

4.1. Synchrotron emission from inhomogeneous sources

The general formulae governing synchrotron emission can be found in e.g. Pacholczyk (1970, Chap. 3 and references therein). For an optically thin source and neglecting circular polarisation the radiation can be described by means of the Stokes parameters I, Q, U governed by the equations

$$\frac{dI}{d\ell} = \epsilon, \tag{7}$$

$$\frac{dQ}{d\ell} = -f\ U - p\ \epsilon\ \cos 2\chi, \tag{8}$$

$$\frac{dU}{d\ell} = f\ Q - p\ \epsilon\ \sin 2\chi, \tag{9}$$

where ℓ is the distance along the line of sight. Here ϵ is the total synchrotron emissivity which for an isotropic power law distribution of relativistic electrons with index γ is given by

$$\epsilon = c_1\ n_{\rm rel}\ B_\perp^{(\gamma+1)/2}\ \lambda^{(\gamma-1)/2}, \tag{10}$$

and f is the rate of Faraday rotation

$$f = c_2\ \lambda^2\ n_{\rm e}\ B_\parallel. \tag{11}$$

The field components perpendicular and parallel to the line of sight are $B_\perp$ and $B_\parallel$ and χ is the angle between the perpendicular field and the node line of the galaxy. λ is the radio wavelength, $n_{\rm e}$ the thermal electron density, $n_{\rm rel}$ the density of relativistic cosmic ray electrons and c_1 and c_2 known constants. p is the degree of polarisation of the emitted radiation. Due to the presence of small-scale random magnetic fields p will be smaller than the theoretically maximal value $(3\gamma+3)/(3\gamma+7)$ valid for an ordered field. (The existence of small-scale fields is essential for a mean-field dynamo to work.)

The solution to Eqs. (7)-(9) is

$$I = \int_{-\infty}^{\infty} \epsilon\ d\ell, \tag{12}$$

$$Q = -\int_{-\infty}^{\infty} p\,\epsilon\ \cos(2\chi + F)\ d\ell, \tag{13}$$

$$U = -\int_{-\infty}^{\infty} p\,\epsilon\ \sin(2\chi + F)\ d\ell, \tag{14}$$

where F is the Faraday depth

$$F(\ell) = \int_{\ell}^{\infty} f(\ell')\ d\ell'. \tag{15}$$

(F is non-dimensional.) The observer is located at $\ell = +\infty$.

Numerical calculations of polarised emission based on these equations have been performed by Cioffi & Jones (1980) for a spherical region with a homogeneous magnetic field, allowing for large values of the Faraday depth F. In observed galaxies the internal Faraday depolarisation is not large, so we make the approximation $F \ll 1$ in (12)-(14), although this may be questionable for 20 cm waves.

Thus we can write

$$Q = Q_0 + \lambda^2 Q_1, \tag{16}$$

$$U = U_0 + \lambda^2 U_1, \tag{17}$$

where

$$Q_0 = -\int_{-\infty}^{\infty} p\,\epsilon\ \cos 2\chi\ d\ell, \tag{18}$$

$$U_0 = -\int_{-\infty}^{\infty} p\,\epsilon\ \sin 2\chi\ d\ell, \tag{19}$$

$$\lambda^2 Q_1 = \int_{-\infty}^{\infty} p\,\epsilon\ \sin 2\chi\ F\ d\ell, \tag{20}$$

$$\lambda^2 U_1 = -\int_{-\infty}^{\infty} p\,\epsilon\ \cos 2\chi\ F\ d\ell. \tag{21}$$

The predicted distribution of polarised emission and Faraday rotation is obtained from these Stokes parameters. In practice one

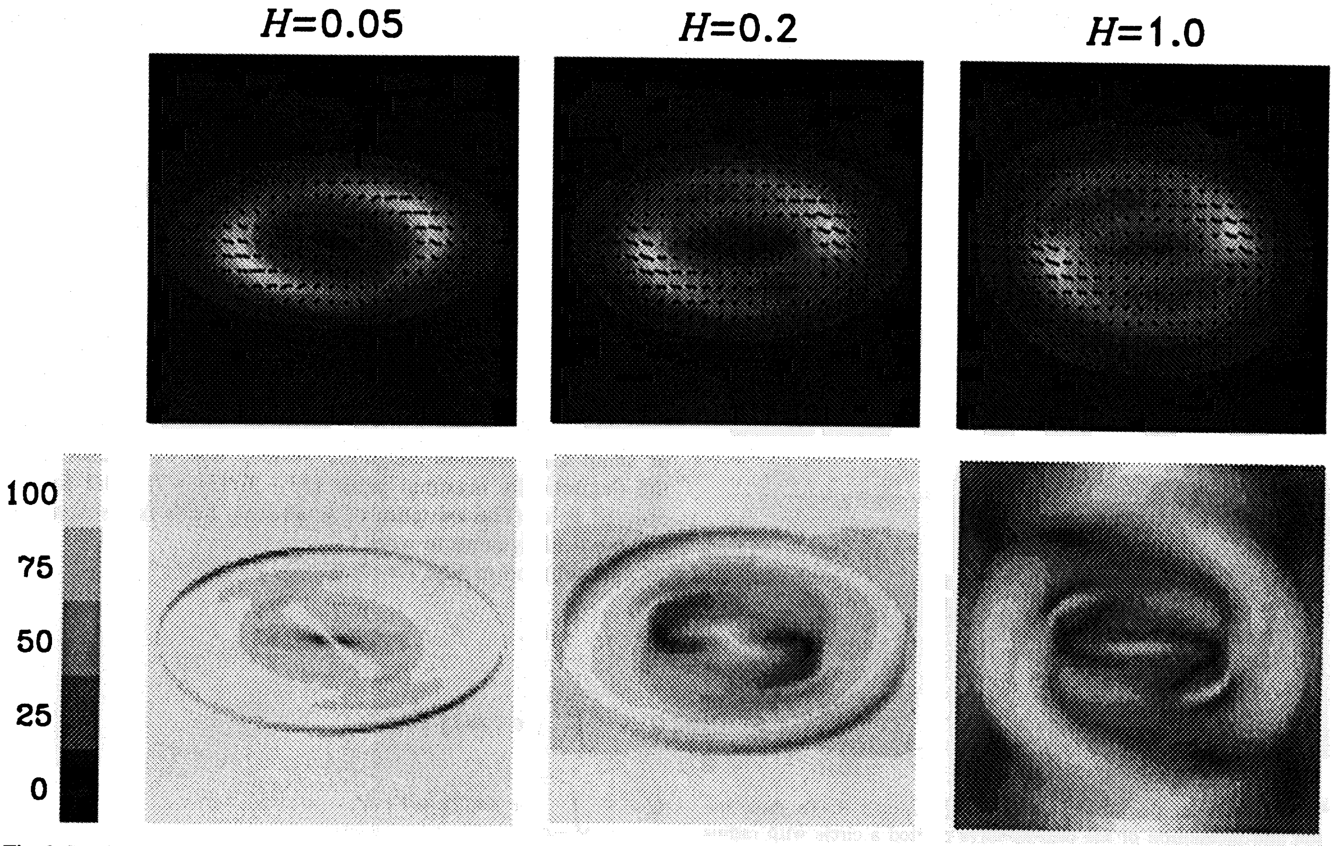

Fig. 6. Synthetical polarisation maps for the S0 mode computed for different values of $H_{\rm rel}$. $i = 60°$. The upper row is a grey scale representation of the total intensity I. The short lines in this map show the field orientation as inferred from the integrated Stokes parameters. The length of these lines is proportional to the polarised intensity. The lower row gives a grey scale representation of the degree of polarisation relative to its value for a homogeneous field. The strip on the left-hand side gives the calibration of the grey scale in per cent

observes the polarisation angle χ_F at two different wavelengths and determines then the rotation measure $\Delta\chi_F/\Delta\lambda^2$. With this definition of the rotation measure we obtain

$$\mathrm{RM} = (Q_1 U_0 - U_1 Q_0)/(Q_0^2 + U_0^2), \tag{22}$$

which can be computed from (18)-(21).

4.2. Synthetic polarisation maps

A detailed map of the polarisation expected in our models requires the specification of the distribution of thermal and of relativistic electrons. However, the quantities $n_{\rm e}$ and $n_{\rm rel}$ are not well determined observationally and may be expected to be strongly inhomogeneous. In view of these difficulties we present theoretical polarisation maps assuming parabolic profiles for $n_{\rm e}$ and $n_{\rm rel}$ with different half-widths $H_{\rm e}$ and $H_{\rm rel}$, respectively. Large values of $H_{\rm e}$ and $H_{\rm rel}$ should exaggerate effects due to extended vertical fields. We use the value $\gamma = 2.4$ for the index of the electron energy distribution (Gioia et al., 1982).

We present our results in a form directly comparable with the observations. Synthetic maps for the S0 mode for different values of $H_{\rm rel}$ are shown in Fig. 6. The upper row of panels shows the total intensity (grey scale map) and the polarised intensity and field orientation (vectors). The lower row of panels shows the degree of polarisation $(Q^2+U^2)^{1/2}/I$. We have set $p=1$, i.e. the figure shows the depolarisation due to variations of the mean

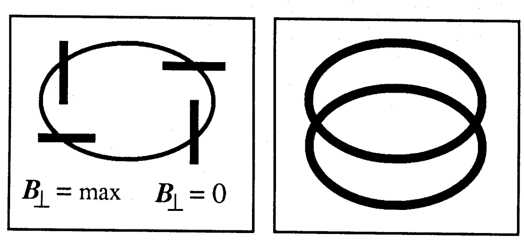

Fig. 7. Geometry of the synchrotron emitting region for the S0 mode. *Left*: For a thin emitting layer the field in the disc plane determines the emission, which is maximal where the field is along the major axis. *Right*: For an extended electron distribution most of the emission arises in two field belts above and below the equatorial plane

field along the line of sight. The sharp ring visible at the edge of the the halo is an artefact of the sharp transition from low conductivity to a perfect vacuum assumed in our model.

In order to understand these maps, consider first the leftmost panels, $H_{\rm rel} = 0.05$. In this case the field in the emitting region is essentially determined by the field in the disc plane, shown in Fig. 4. The strongest emission comes from the ring where the field is strongest and in this ring from the sections where the perpendicular component of the field is largest. Since the vertical field is zero in the disc plane, this corresponds to the points where the field is along the projected major axis. This is shown in the left panel of Fig. 7 giving a schematical sketch of the

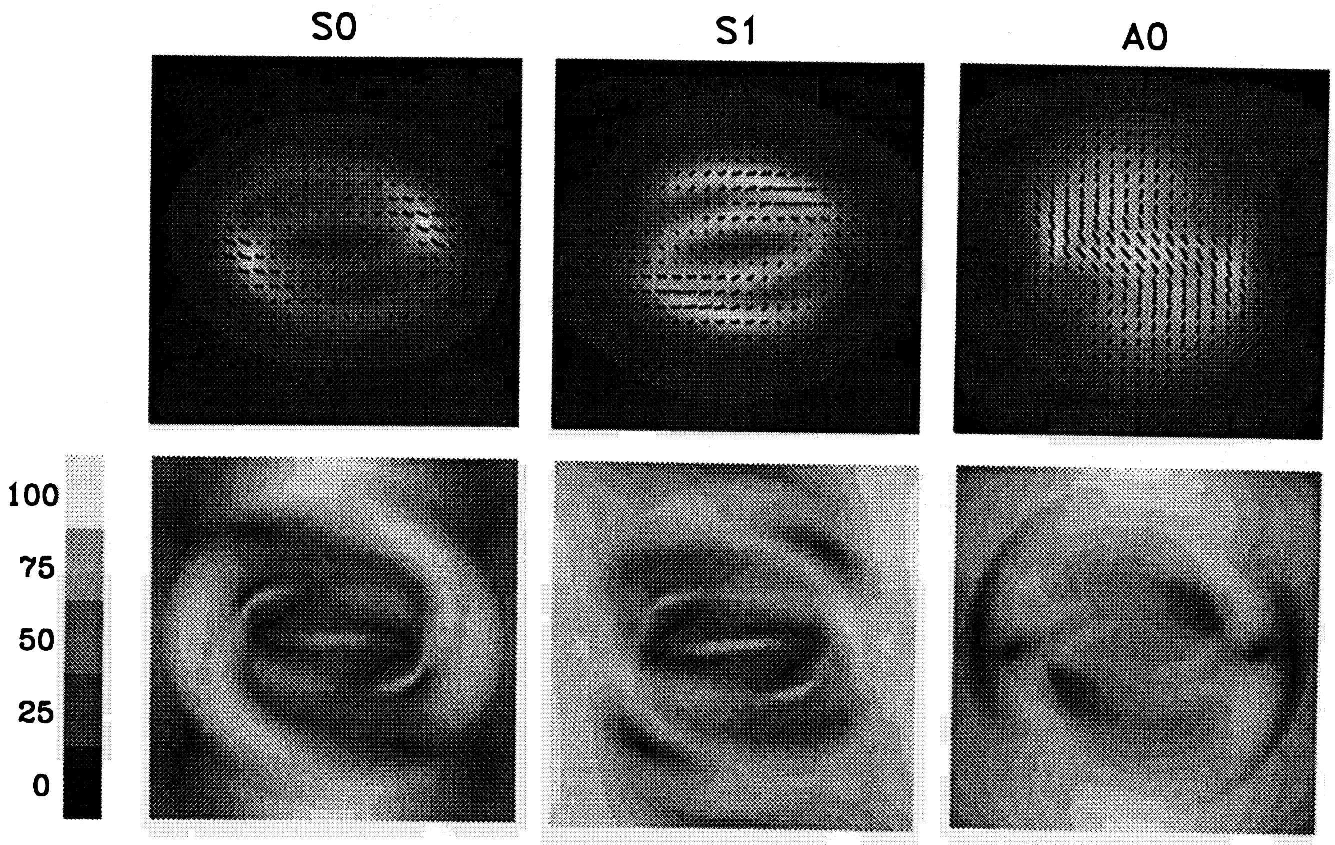

Fig. 8. Same as Fig. 6 for S0, S1, and A0 modes of model R computed for $H_{\rm rel} = 1$. $i = 60°$

field geometry of the emitting region. Since the field is effectively homogeneous, the depolarisation is small.

In the rightmost panels of Fig. 6 the relativistic electrons fill most of the galaxy and the emission represents a projection of the field strength in the whole galaxy. The fields are largest in two rings on both sides of the plane (see Fig. 2) and the total emission can be seen as a superposition of these. This is illustrated in the right panel of Fig. 7. As before, intensity maxima are displaced from the major axis, giving a the impression of a non-axisymmetric field distribution. There are large variations in the field orientation along the line of sight, leading to correspondingly large and variable depolarisation.

Polarisation maps for the three modes S0, S1, and A0 are shown in Fig. 8. The general distribution of intensity and polarisation for the S1 and A0 modes can be understood on the basis of similar considerations as for the S0 mode. Remarkably complex patterns are produced when the synchrotron emitting regions are extended. We can find no simple criteria that would allow one to make inferences about the magnetic field geometry on the basis of intensity distributions alone.

In Fig. 9 we give maps for the S1 mode at various inclinations, and in Fig. 10 we show the effect of various orientations ϕ_0 of the line of nodes. These maps further emphasise the great variety of patterns that can be produced in these very simple models by the combined effects of projection and anisotropic emission.

4.3. Synthetic rotation measures

The crucial distinction between ASS and BSS fields is in the behaviour of the rotation measure RM as a function of azimuthal angle. We are interested in whether the doubly periodic nature of RM characteristic of BSS fields remains valid when the field extension into the halo is taken into account. In this section we investigate possible modifications of the RM curves due to the finite field extension into the galactic halo.

In Fig. 11 we plot the rotation measure for the S1 mode for various inclinations using different values of $H_{\rm e}$. In general $H_{\rm e}$ will not be the same as $H_{\rm rel}$, but here we only consider the case where they are equal. We present RM normalised with $c_2 n_{\rm e} L B_{\rm max}$. For comparison we also show the total rotation measure $\mathrm{RM_{tot}}$ defined as

$$\mathrm{RM_{tot}} = \int_{-\infty}^{\infty} c_2 n_{\rm e} B_{\parallel} d\ell, \qquad (23)$$

which represents the total amount of Faraday rotation through the galaxy. For inclinations larger than about 30°the familiar doubly periodic dependence is found. However, for smaller inclinations the rotation measure is dominated by the vertical field, and consequently only a single maximum is obtained. Thus the rotation measure method cannot detect bisymmetric fields in small-inclination systems.

In Fig. 12 we compare the rotation measures for the axisymmetric modes S0 and A0 for different values of $H_{\rm e}$. The basic behaviour is singly periodic for S0 and doubly periodic for A0. However, there are strong and rapid variations in RM that make an interpretation of the field geometry in terms of simple sinusoidal dependences hazardous.

While we do confirm that a doubly periodic variation of RM is a reliable criterion for a bisymmetric spiral, we would like

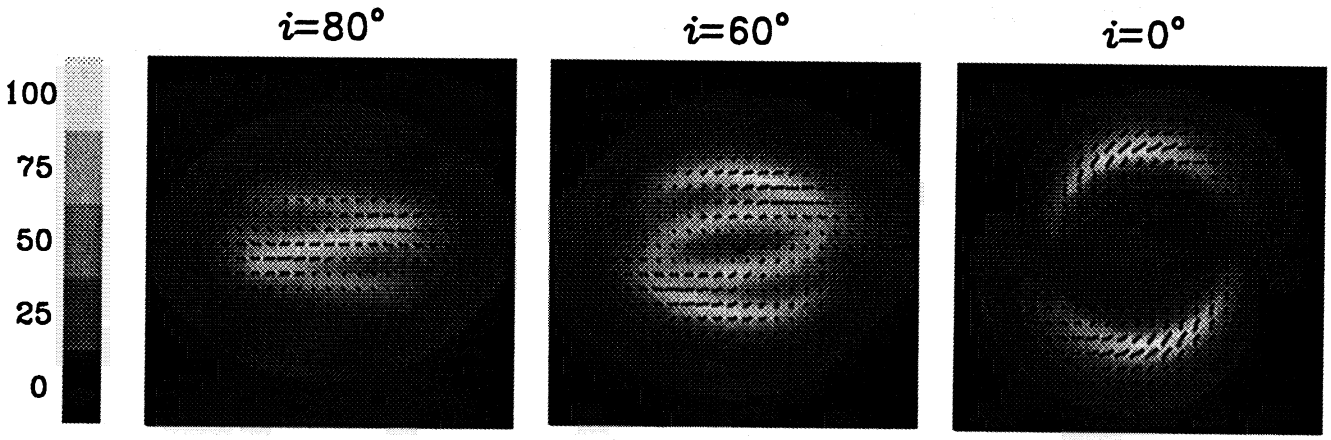

Fig. 9. Intensity and polarisation maps for the S1 mode at various inclinations (i=0°, 60°, 80°). $H_{\rm rel}=1$. Otherwise the same as Fig. 6

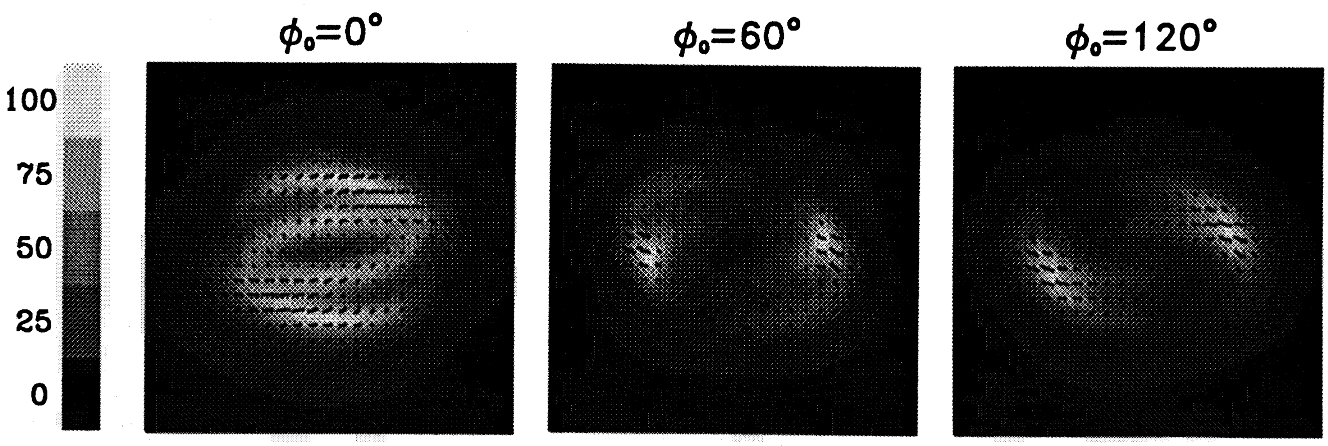

Fig. 10. Intensity and polarisation maps for the S1 mode at various orientations ϕ_0 of the line of nodes. (The map for $\phi_0 = 0°$ is also included in Figs. 8 and 9.) $H_{\rm rel} = 1$. $i = 60°$. Otherwise the same as Fig. 6

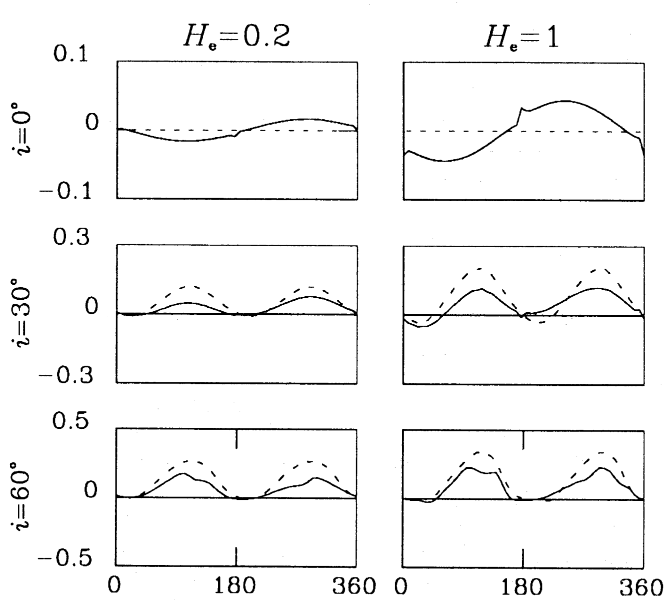

Fig. 11. The dependence of the rotation measure RM on inclination and H_e (= $H_{\rm rel}$) for the S1 mode. $\phi_0 = 0°$. The dotted lines give the variation of $\rm RM_{tot}$. The variation of RM with azimuthal angle is plotted along a circle of radius 0.6 in the galactic plane (corresponding to an elliptic path in the sky)

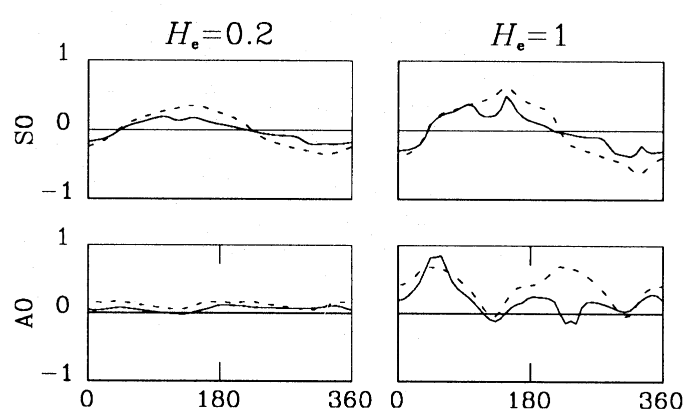

Fig. 12. RM for the S0 and A0 modes for two values of H_e. $i = 60°$. Otherwise the same as Fig. 11

to emphasise that the variations of RM may be quite complex even in very simple models and that the interpretation of RM observations requires some care.

5. Conclusions

We have considered magnetic field configurations predicted from kinematic mean-field dynamo theory. Investigating possible dynamo models for galaxies we find that central magnetic fields are expected to be dipolar. Such a field is generated mainly by an α^2 mechanism operating in the central part of the galactic disc. The field is strongly concentrated toward the centre and the field lines go straight through the middle. The similarity to jet-like emission features at the centre of the Milky Way suggest that an explanation in terms of dynamo generated fields should not be *a priori* excluded. The observed filaments could be produced by the injection of relativistic electrons into some of the flux tubes passing close to the galactic centre.

We have also considered models where the central A0 modes are suppressed. We find that in this case the S0 and S1 modes are similar to observed galactic fields. We also find that these modes may extend into the galactic halo, and that therefore fields observed far away from the disc need not necessarily have been carried there by a galactic wind.

For a real comparison between observation and theory one has to compute synthetical polarisation maps for the Stokes parameters I, Q, and U. These quantities contain contributions from all locations in the galaxy and can therefore be strongly affected when the fields extend with considerable strength into the halo. The models we have presented show the effects to be expected in that case. In particular the curves of the rotation measure show additional peaks and the dependence of RM on azimuthal position is no longer sinusoidal. Still, the extent of these deviations is not really large enough to change the customary interpretation in terms of ASS and BSS. Thus, we find that the criterion based on rotation measures is mostly quite reliable.

Our results should not be strongly dependent on the adopted model. In general we find that even neutral or slightly damped modes become concentrated within a limited region where the amplification is strongest (cf. Starchenko & Shukurov 1989). With an α effect that is antisymmetric with respect to the disc plane one thus expects that a field structure consisting of two belts on both sides of the plane will be quite general. Only the exact position of the belts will depend on the model. It would be interesting to see, whether this kind of structure could be detected in some galaxies.

We are certainly still quite far away from realistically modelling the magnetic field generation in galaxies. One important fact that our models do not account for is the apparent alignment of magnetic field lines with the spiral arms. This would require a theory that accounts for the effects of density waves on the magnetic field. Observations indicate that the compression factor in spiral arms is at least 2-4 (Elmegreen & Elmegreen 1984). Even neglecting the effects of density waves on the field, variations of the densities of relativistic and thermal electrons in spiral arms will affect the interpretation of observations (cf. Krause et al., 1989a, Appendix). In addition, variations in the degree of randomness of the field are likely to be important (Sukumar & Allen, 1989).

Finally, we wish to stress that the usual derivations of equations for the mean magnetic field are not really applicable in galaxies. In particular, the theory of how the α effect and turbulent magnetic diffusivity are affected by the spiral structure is not developed yet. It may be rash to adopt *ad hoc* models such as a sinusoidal modulation of the α effect without a proper dynamical basis.

References

Allen, R.J., Sukumar, S., Hu, F.X., van der Kruit, P.C.: 1990, in *Galactic and Intergalactic Magnetic Fields*, IAU *Symp. 140*, eds. R. Beck, P. Kronberg, R. Wielebinski, Kluwer, Dordrecht

Baryshnikova, Y., Ruzmaikin, A.A., Sokoloff, D.D., Shukurov, A.: 1987, *Astron. Astrophys.* **177**, 27

Beck, A.: 1990, *Geophys. Astrophys. Fluid Dyn.* **50**, 3

Brandenburg, A., Tuominen, I., Krause, F.: 1990, *Geophys. Astrophys. Fluid Dyn.* **50**, 95

Chiba, M., Tosa, M.: 1990, in *Galactic and Intergalactic Magnetic Fields*, IAU *Symp. 140*, eds. R. Beck, P. Kronberg, R. Wielebinski, Kluwer, Dordrecht

Cioffi, D.F., Jones, T.W.: 1980, *Astron. J.* **85**, 368

Donner, K.J.: 1990, in *Galactic and Intergalactic Magnetic Fields*, IAU *Symp. 140*, eds. R. Beck, P. Kronberg, R. Wielebinski, Kluwer, Dordrecht

Donner, K.J., Brandenburg, A.: 1990a, *Geophys. Astrophys. Fluid Dyn.* **50**, 121

Donner, K.J., Brandenburg, A.: 1990b, in *Dynamics of Astrophysical Discs*, ed. J.A. Sellwood, Cambridge University Press, p.151

Elmegreen, D.M., Elmegreen, B.G.: 1984, *Astrophys. J. Suppl.* **54**, 127

Elstner, D., Meinel, R., Rüdiger, G.: 1990, *Geophys. Astrophys. Fluid Dyn.* **50**, 85

Fujimoto, M., Sawa, T.: 1987, *Publ. Astron. Soc. Jpn.* **39**, 375

Gioia, I.M., Gregorini, L., Klein, U.: 1982, *Astron. Astrophys.* **116**, 164

Heiles, C.: 1987, in *Interstellar Processes*, eds. D.J. Hollenbach, H.A. Thronson Jr., Reidel, Dordrecht, p.171

Hummel, E., Lesch, H., Wielebinski, R., Schlickeiser, R.: 1988, *Astron. Astrophys.* **197**, L29

Jennings, R., Brandenburg A., Moss, D., Tuominen I.: 1990, *Astron. Astrophys.* **230**, 463

Krasheninnikova, Yu.S., Ruzmaikin, A.A., Sokoloff, D.D., and Shukurov, A. M.: 1990, *Geophys. Astrophys. Fluid Dyn.* **50**, 131

Krause, F.: 1990, *Geophys. Astrophys. Fluid Dyn.* **50**, 67

Krause, F., Elstner, D., Meinel, R., Rüdiger, G.: 1990, in *Galactic and Intergalactic Magnetic Fields,* IAU *Symp. 140,* eds. R. Beck, P. Kronberg, R. Wielebinski, Kluwer, Dordrecht, p. 97

Krause, M., Hummel, E., Beck, R.: 1989a, *Astron. Astrophys.* **217**, 4

Krause, M., Beck, R., Hummel, E.: 1989b, *Astron. Astrophys.* **217**, 17

Lesch, H., Crusius, A., Schlickeiser, R., Wielebinski R.: 1989, *Astron. Astrophys.* **217**, 99

McKee, C.F., Ostriker, J.P.: 1977, *Astrophys. J.* **217**, 148

Mestel, L., Subramanian, K.: 1990, in *Galactic and Intergalactic Magnetic Fields*, IAU *Symp. 140*, eds. R. Beck, P. Kronberg, R. Wielebinski, Kluwer, Dordrecht

Morris, M., Yusef-Zadeh, F.: 1989, *Astrophys. J.* **343**, 703

Moss, D., Tuominen, I.: 1990, *Geophys. Astrophys. Fluid Dyn.* **50**, 113

Pacholczyk, A.G.: 1970, *Radio Astrophysics*, Freeman, San Francisco

Parker, E.N.: 1971, *Astrophys. J.* **163**, 255

Rädler, K.-H.: 1980, *Astron. Nachr.* **301**, 101

Rädler, K.-H.: 1986, *Plasma Physics*, ESA SP-251, 569

Rädler, K.-H., Bräuer, H.-J.: 1987, *Astron. Nachr.* **308**, 101

Rand, R.J., Kulkarni, S.R., Hester, J.J.: 1990, *Astrophys. J. Letters* **352**, L1
Reynolds, R.J.: 1989, *Astrophys. J. Letters* **339**, L29
Roberts, P.H., Stix, M.: 1972, *Astron. Astrophys.* **18**, 453
Rubin, V.C., Burstein, D., Ford, W.K. Jr., Thonnard, N.: 1985, *Astrophys. J.* **289**, 81
Rüdiger, G.: 1990, *Geophys. Astrophys. Fluid Dyn.* **50**, 53
Ruzmaikin, A., Sokoloff, D., Shukurov, A.: 1988a, *Nature* **336**, 341
Ruzmaikin, A.A., Shukurov, A.M., Sokoloff, D.D.: 1988b, *Magnetic Fields of Galaxies*, D. Reidel & Kluwer Publ.
Sawa, T., Fujimoto, M.: 1986, *Publ. Astron. Soc. Jpn.* **38**, 133
Sofue, Y., Fujimoto, M., Wielebinski, R.: 1988, *Ann. Rev. Astron. Astrophys.* **24**, 459
Sofue, Y., Reich, W., Reich, P.: 1989, *Astrophys. J. Letters* **341**, L47
Starchenko, S.V., Shukurov, A.M.: 1989, *Astron. Astrophys.* **214**, 47
Stepinski, T.F., Levy, E.H.: 1988, *Astrophys. J.* **331**, 416
Stix, M.: 1975, *Astron. Astrophys.* **42**, 85
Sukumar, S., Allen, R.J.: 1989, *Nature* **340**, 537
Tosa, M., Fujimoto, M.: 1978, *Publ. Astron. Soc. Jpn.* **30**, 315
Yusef-Zadeh, F., Morris, M.: 1988, *Astrophys. J.* **329**, 729
Yusef-Zadeh, F., Morris, M., Chance, D.: 1984, *Nature* **310**, 557
Yusef-Zadeh, F., Morris, M., Slee, O.B., Nelson, G.J.: 1986, *Astrophys. J. Letters* **300**, L47

This article was processed by the author using Springer-Verlag TEX AA macro package 1989.